Seismic Structures of the Earth's Inner Core Boundary Beneath the Bearing Sea and Mexico

Dongdong Tian[1] (dongzhi@mail.ustc.edu.cn), Lianxing Wen[2,1]

1. Laboratory of Seismology and Physics of Earth's Interior, University of Science and Technology of China
2. Department of Geosciences, State University of New York at Stony Brook

AGU 2016
DI43A-2657

1. Introduction

The Earth's solid inner core grows from the solidification of the liquid outer core. The solidification process provides driving forces for the thermo-compositional convection in the outer core and power for generating the geodynamo through the release of latent heat and light elements. Thus, the detailed structure of the ICB is the key to the understanding of thermo-compositional state of the inner core and driving forces in outer core convection.

The ICB has been thought to be simple, flat and sharp, due to the presumed extremely small variation in temperature in the outer core. However, recent seismological studies have suggested complex ICB structures, which exihibits localized temporal and spatial changes.

In this research, we use pre-critical PKiKP and PcP phases, compressional waves that are reflected off the Earth's ICB and core-mantle boundary (CMB) respectively, to constrain the detailed seismic structure of the ICB. We performed a systematic search of events from 2004 to 2015 recorded by USArray, and collected 9 events with 607 high-quality PKiKP-PcP observations. The data sample two ICB regions beneath the Bearing Sea and Mexico. We will present seismic constraints of these two regions based on observations of PKiKP-PcP differential travel time residuals, PKiKP/PcP amplitude ratios and PKiKP-PcP waveform differences.

2. Data and Methods

Pre-critical PKiKP phases in the distance from 0° to 90°, are very sensitive to topography, geometry and properties contrasts across the ICB. However, PKiKP phases are usually weak and obscured by seismic coda and noise, making it difficult to be routinely detected.

We search the records from USArray stations (black triangles in Fig. 1b) in 2004 to 2015, and collect 9 events (red stars in Fig. 1b) with high-quality PKiKP (red lines in Fig. 1a) and PcP phases (blue lines in Fig. 1a). The PcP phase is used as a reference phase, which has a similar raypath as PKiKP phase in crust and upper mantle (Fig. 1a).

We handpick arrival times of PKiKP and PcP phases and recheck using cross-correlation technique, then calculate the PKiKP-PcP differential travel time residual with respect to PREM model, defined as $\Delta T^{Res} = (T^{obs}_{PKiKP} - T^{pre}_{PKiKP}) - (T^{obs}_{PcP} - T^{pre}_{PcP})$. The use of differential PKiKP-PcP travel time residual minimizes the effects of shallow Earth's structure and uncertainties in event origin time, location and can be used to constrain the topography of the ICB.

PKiKP/PcP amplitude ratios, which minimize the effects of shallow Earth's structure, source magnitude and radiation pattern, are sensitive to the properties contrasts across the ICB. Due to the complicated perturbations, PKiKP/PcP amplitude ratios show a large mount of scattering. We thus bin the amplitude ratios in sliding windows of different size.

We aslo stack PcP and PKiKP waveforms along the picked arrival times in geographical bins based on PKiKP reflection points. Due to the similar take-off angles from the seismic source and similar incident angles to the reciever between PcP and PKiKP phases, the study of their waveform differences provide tight constraints on the fine-scale structure in the vicinity of the ICB.

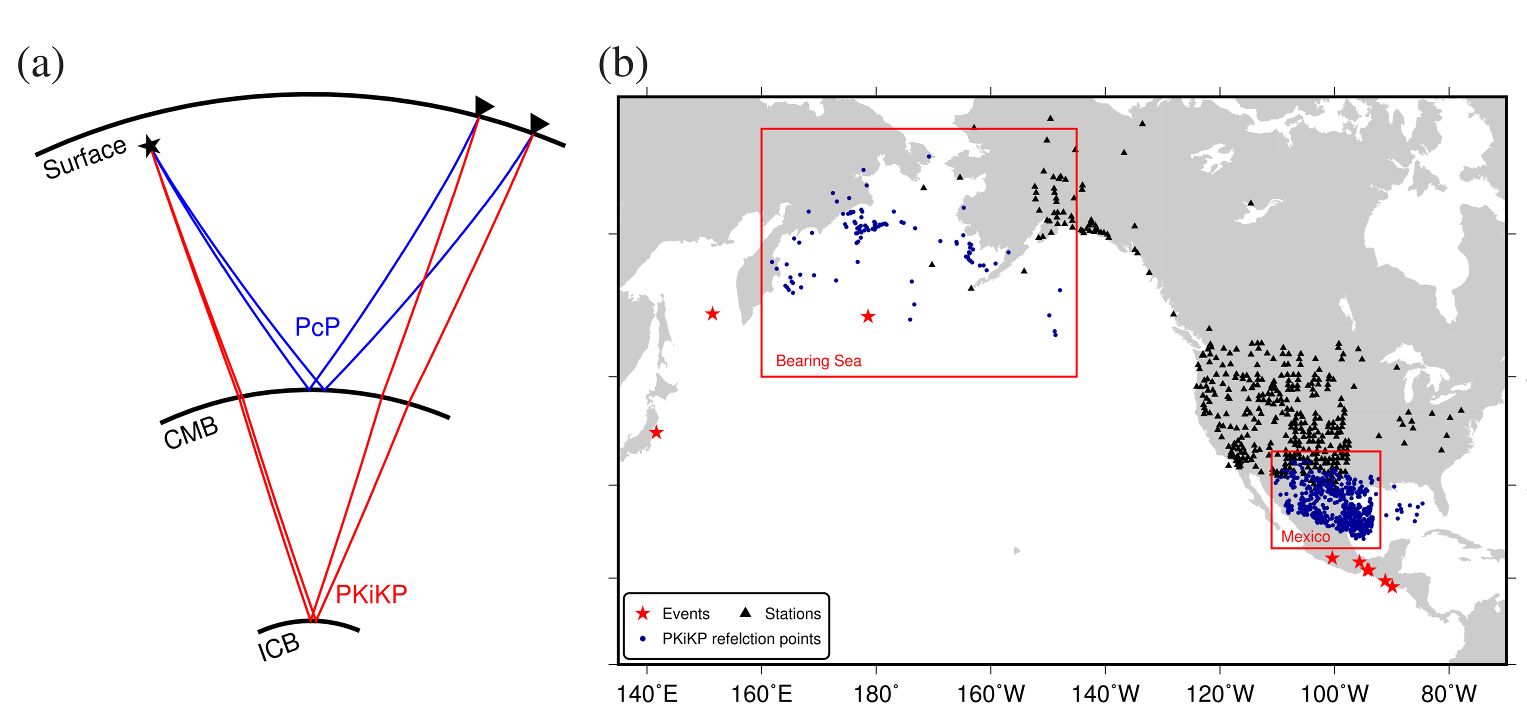

Fig. 1. *(a) Ray paths of PKiKP (red) and PcP (blue) phases for a seismic source at a depth of 300 km (black star) and receivers (black triangles) at two example epicentral distances of 30° and 35°. (b) Map view of seismic events (red stars) recorded by USArray stations (black triangles) used in this research. The PKiKP reflection points at the ICB are also plotted (blue dots).*

3. ICB Beneath Mexico

In this section, we present seismic observations which sample ICB region beneath Mexico. The PKiKP-PcP differential travel time residuals exhibits large spatial variations from -1.0 s to 1.0 s in a horizontal distance of about 5° (Fig. 2).

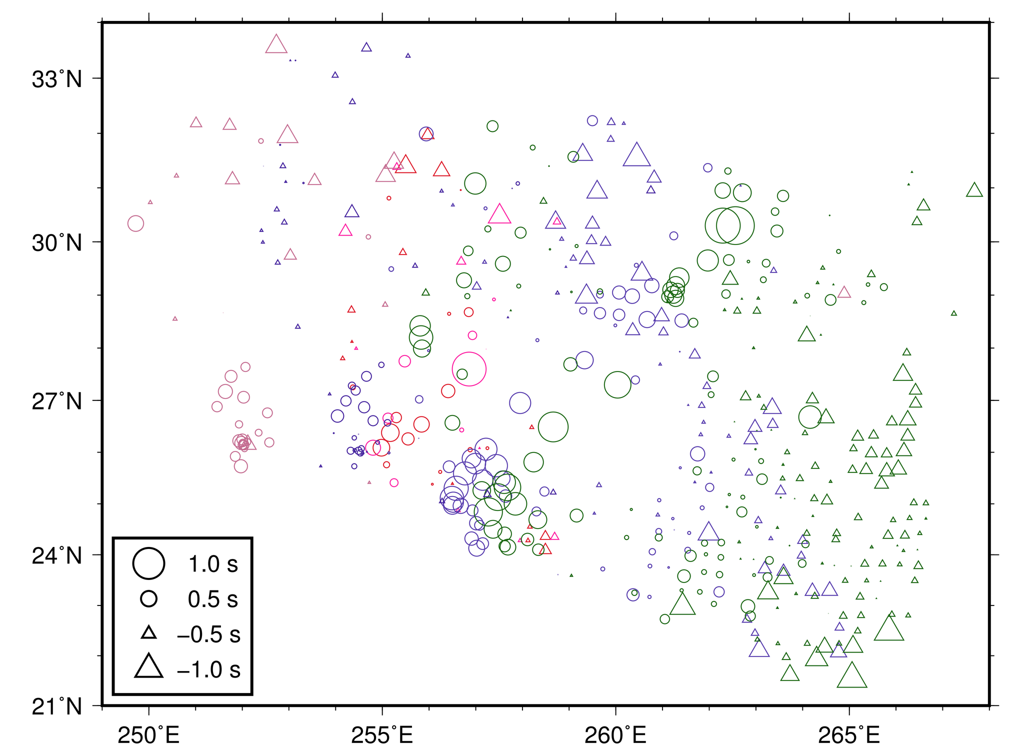

Fig. 2. *PKiKP-PcP differential travel time residuals with respect to PREM, plotted at the PKiKP reflection points at the ICB. Events are coded using different colors. Residuals for each event are plotted using circles (positive residuals) and triangles (negative residuals) with different size. Note that a mean residual of 0.6 s is removed from all observed PKiKP-PcP differential travel time residuals for better clarity.*

The PKiKP-PcP differential travel time residuals have a positive correlation with PKiKP travel time residuals (Fig. 3a), while no correlation is found with PcP travel time residuals (Fig. 3b), implying that the large variations of PKiKP-PcP residuals mainly come from PKiKP phases. A typical ULVZ model of a 10% decrease in P wave velocity over a 15 km layer near the PKiKP entrant or exit points at the CMB, gives a travel time pertubation of about 0.12 s, which is not quite large enough to account for the observed variation of 1.0 s. Thus, the observed PKiKP-PcP differential travel time residuals may indicate a ICB topographic change of 5 km.

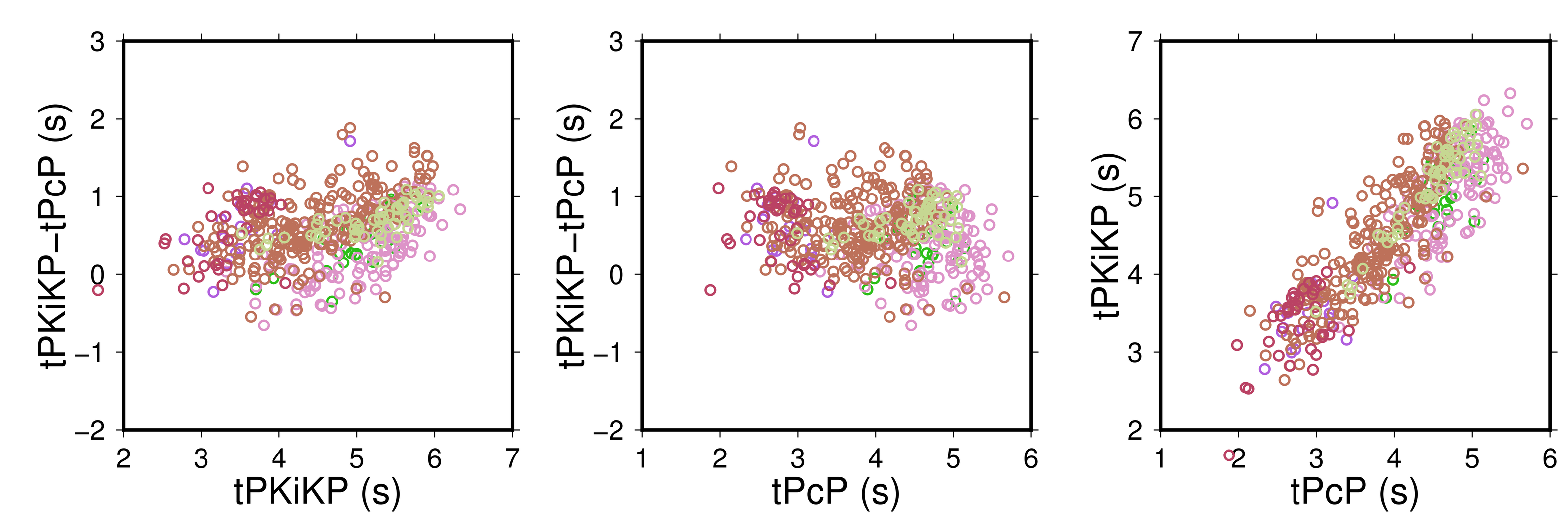

Fig. 3. *Relationship among PKiKP-PcP differential travel time residuals, PKiKP travel time residuals and PcP travel time residuals. Events are coded using different colors.*

The binned PKiKP/PcP amplitude ratios exhibit much larger values than predictions of different ICB models (Fig. 4) and spatial variations (Fig. 5).

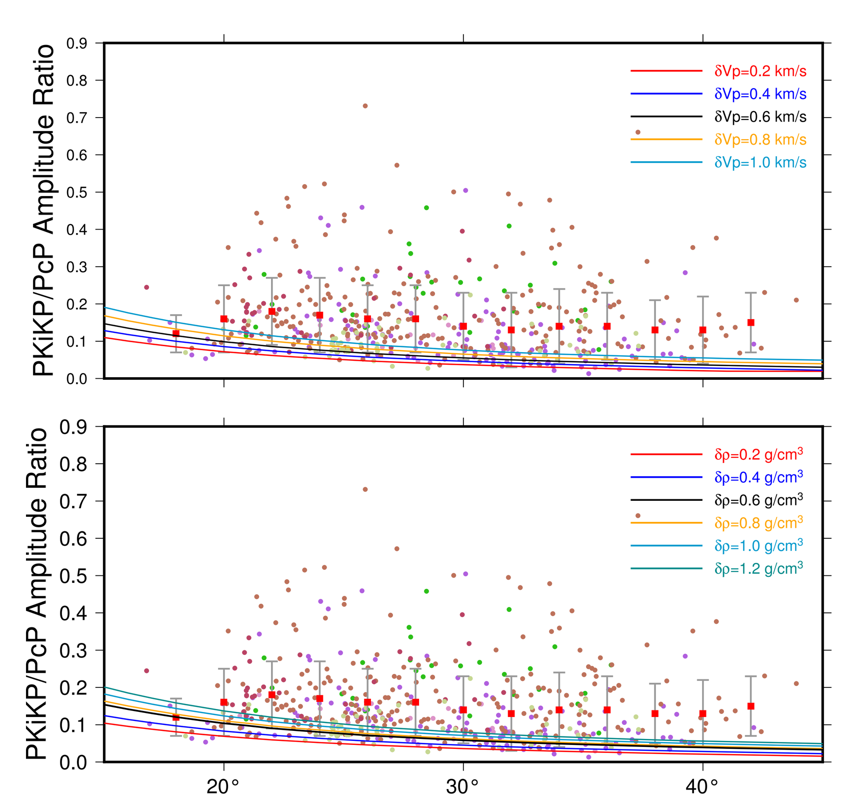

Fig. 4. *Observed PKiKP/PcP amplitude ratios (dots) as a function of epicentral distance, with predictions (lines) of different P wave speed (a) and density (b) constrasts across the ICB. The red squares represent average amplitude ratios of each bins, and the error bar represent standard deviations.*

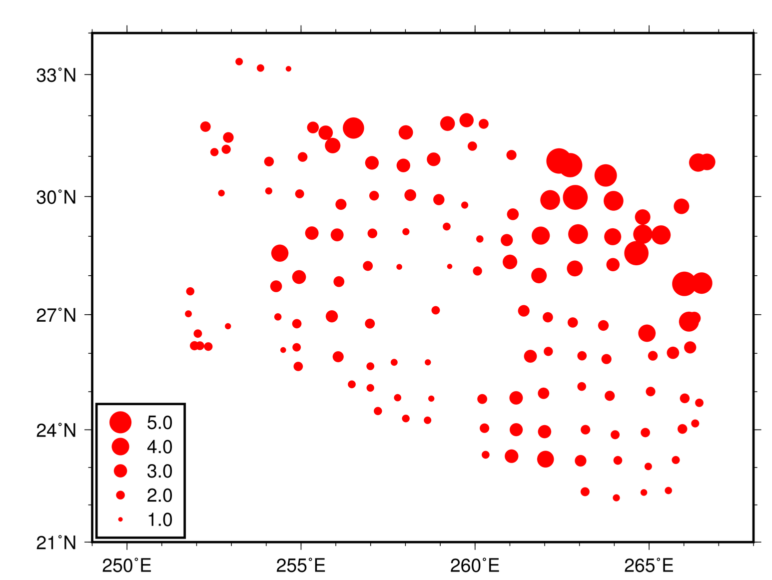

Fig. 5. *Binned PKiKP/PcP amplitude ratio residuals, defined as the ratio between observed and predicted PKiKP/PcP amplitude ratios. 1° geographical bins with the bin centers shift by 1° in latitude and longtitude are used. The ratio residuals are plotted at the mean PKiKP reflection locations in each bins.*

4. ICB Beneath the Bearing Sea

In this section, we present seismic observations which sample the ICB region beneath Bearing Sea (Fig. 1b). The small variations of the PKiKP-PcP differential travel time residuals indicate a flat ICB in this region (Fig. 6).

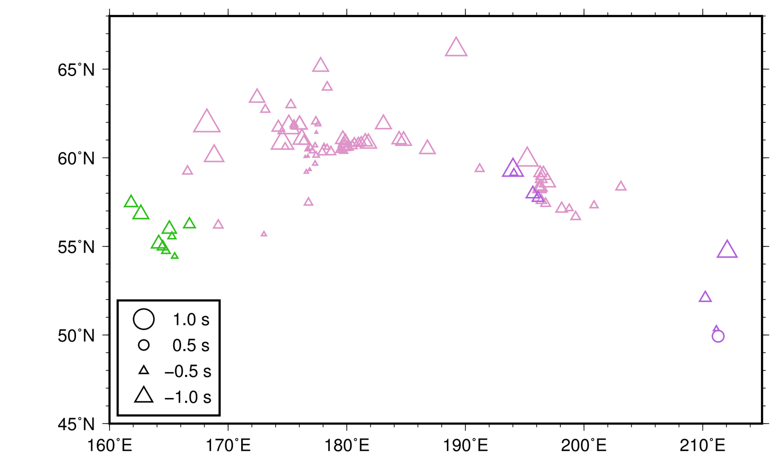

Fig. 6. *PKiKP-PcP differential travel time residuals with respect to PREM, plotted at the PKiKP reflection points of the ICB. Events are coded using different colors. Residuals for each event are plotted using circles (positive residuals) and triangles (negative residuals) with different size.*

The linear relationship between PKiKP and PcP travel time residuals (Fig. 7) indicates that most variations in PKiKP and PcP travel time residuals originate from shallow Earth's hetergeneity, which can be effectively eliminated by using PKiKP-PcP differential travel time residuals.

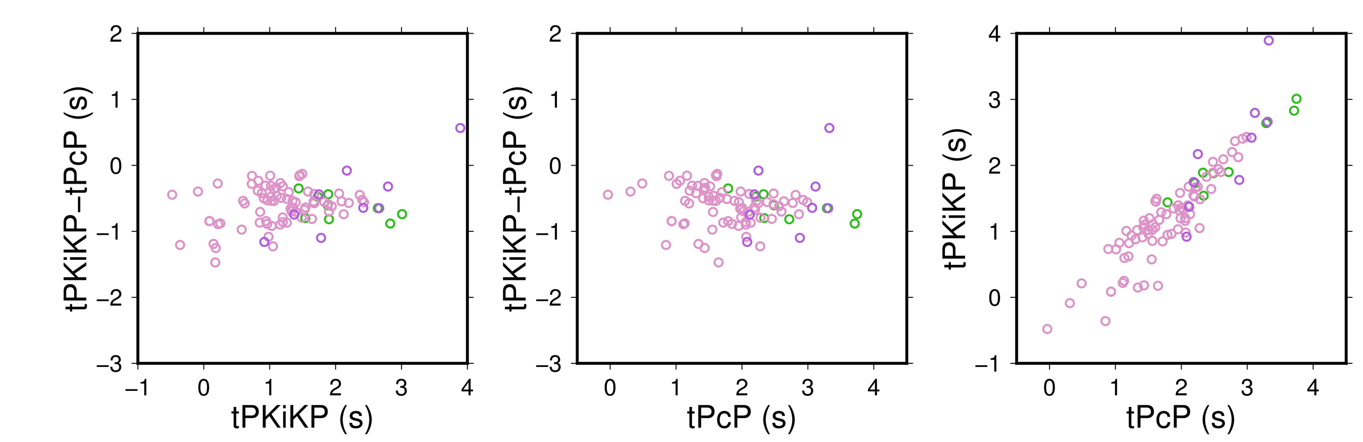

Fig. 7. *Relationship among PKiKP-PcP differential travel time residuals, PKiKP travel time residuals and PcP travel time residuals.*

The stacked PKiKP and PcP waveforms show similar waveforms (Fig. 8), indicating a sharp interface at both the CMB and ICB. The PKiKP/PcP amplitude ratios exhibit large scattering on single records. The PKiKP/PcP amplitde ratios binned by epicentral distance, exhibit much larger amplitude ratios than predictions of different ICB models (Fig. 9).

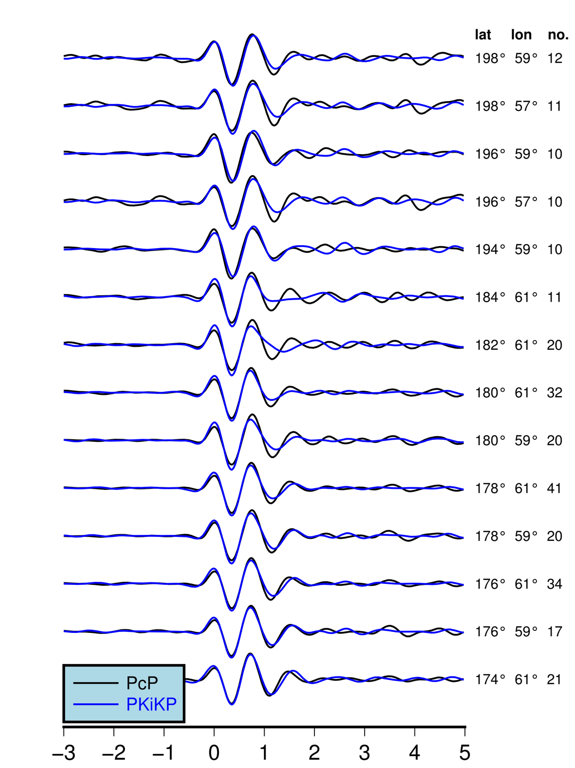

Fig. 8. *Comparisons of stacked PKiKP (blue) and PcP (black) waveforms in each geographical bins. The locations of the bins center and the number of traces used in each stacking are labeled at the right of each traces.*

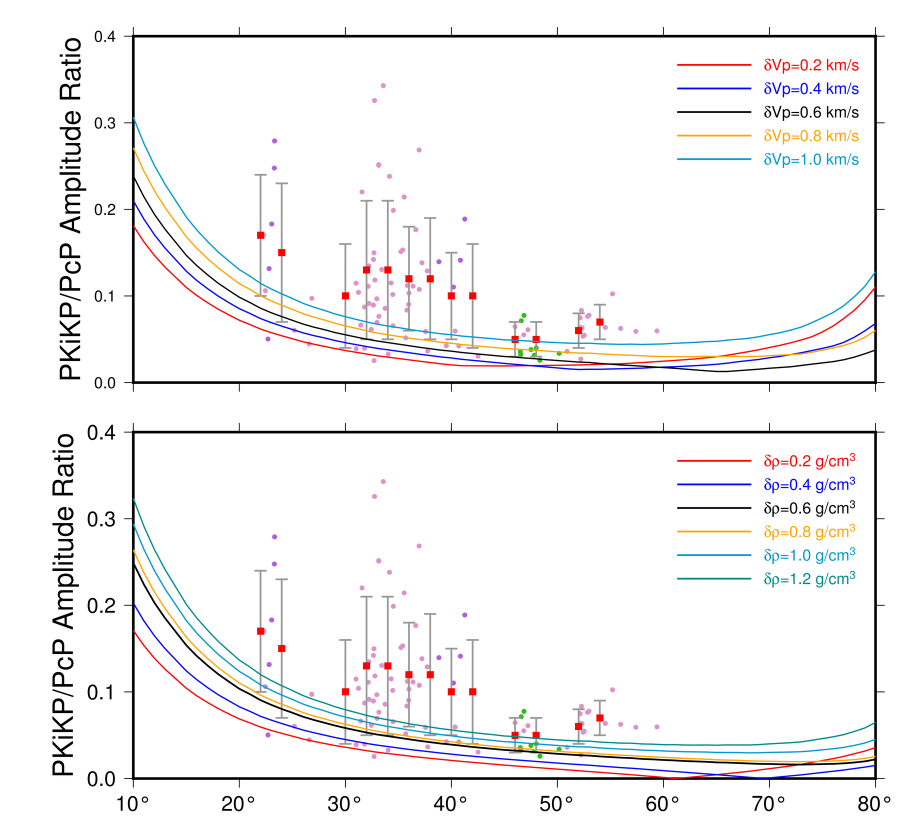

Fig. 9. *Observed PKiKP/PcP amplitude ratios (dots) as a function of epicentral distance, with predictions (lines) of different P wave speed (a) and density (b) constrasts across the ICB. The red squares represent average amplitude ratios in each bins, and the error bar represnt standard deviations.*

5. Conclusions

We collect a large dataset of high-quality PKiKP waveforms, and use PKiKP-PcP differential travel time residuals, PKiKP/PcP amplitude ratios, and PKiKP-PcP waveform differences to constrain ICB properties. Based on the observations, the ICB beneath Bearing Sea has a sharp and flat boundary, and the ICB beneath Mexico may have a bumpy ICB with a topographic height change of 5 km. PKiKP/PcP amplitude ratios are much larger than predictions, implying possible other factors which affects the amplitude ratios.